# Isomeric States of Po Isotopes in the Nanosecond Range Populated by Pb($\alpha$, $xn$) Reactions*

T. YAMAZAKI

*Lawrence Radiation Laboratory, University of California, Berkeley, California 94720 and Department of Physics, University of Tokyo, Bunkyo-ku, Tokyo, Japan*

(Received 27 May 1969)

Isomeric states of Po isotopes from $A=204$ to $A=211$ have been investigated by means of the nanosecond time analysis of Pb($\alpha$, $xn$) $\gamma$ rays produced in natural beam bunches of a cyclotron. In addition to those already reported, new isomeric states have been revealed systematically. The following half-lives have been measured: $^{204}$Po: 190±20 nsec; $^{206}$Po: 160±40 nsec; $^{208}$Po: 380±100 nsec; and $^{210}$Po: 110±10 nsec. The possibility that such half-lives are associated with the expected 8+ state of predominant configuration $h_{9/2}{}^2(p)$ is discussed. Another half-life (24 nsec) found in $^{210}$Po was assigned as a $(h_{9/2}i_{13/2})$ 11− isomeric state. Odd isotopes show three-particle isomeric states in addition to the $i_{13/2}(n)$ isomeric state. Several characteristic features revealed in this study are discussed.

## I. INTRODUCTION

In this paper, we shall report on a survey study of isomeric states of Po isotopes ($Z=84$) from $A=204$ to 211 and relevant low-lying levels populated by Pb($\alpha$, $xn$) reactions. The method of the nanosecond time analysis of reaction $\gamma$ rays utilizing natural beam bunches of a cyclotron, as developed by Yamazaki and Ewan,[1,2] was employed. This method has recently been applied to Sn isotopes.[3,4]

In Ref. 1, new isomeric states of $^{210}$Po resulting from proton orbits of large $j$ have been reported. These states attracted much attention from the shell-model point of view. Combined with a preliminary measurement of $g$ factors of these high-spin isomeric states, a discussion of the electric and magnetic core polarization was made by Yamazaki.[5] Treytl, Hyde, and Yamazaki[6] studied levels of $^{208}$Po in detail from the decay of $^{208}$At and also with the in-beam spectroscopy and interpreted a 380-nsec isomeric state as the 8+ member of the $h_{9/2}{}^2$ proton configuration also appearing in $^{210}$Po. The occurrence of the $(h_{9/2}{}^2)$8+ isomeric state in $^{208}$Po arises from the fact that this state lies lower than neutron states of the same spin, which helps retain the unique character of the $(h_{9/2}{}^2)$8+ state. Yamazaki and Matthias[7] observed a 100-nsec isomeric state in $^{209}$Po. They measured the $g$ factor of this state and concluded that it must be a three-particle state of the $(h_{9/2}{}^2(p))$8+, $p_{1/2}(n)$ configuration. This is an interesting example to show the occurrence of the $(h_{9/2}{}^2)$8+ isomeric state in odd-mass nuclei as well.

There was some previous information on long-lived isomeric states. Isomeric states of $^{205}$Po and $^{207}$Po were studied by Hargrove and Martin.[8] High-spin $\alpha$-decaying isomeric states of $^{211}$Po and $^{212}$Po were studied by Perlman *et al.*[9]

It was our aim to survey unknown region of Po isotopes. The present work has established isomer and level systematics in even and odd Po isotopes down to $^{204}$Po.

## II. EXPERIMENTAL PROCEDURES

### A. Experimental Arrangements

The experimental arrangements employed in the present work are almost the same as that reported in detail in Ref. 4. Here we shall describe the experimental procedures briefly. The $\alpha$-particle beam from 24 to 50 MeV from the Berkeley 88-in. sector-focused cyclotron was transported into a scattering chamber to bombard Pb targets to yield Pb($\alpha$, $xn$)Po $\gamma$ rays.

The $\gamma$ rays were detected with a Ge(Li) detector. In most cases a 30-cm$^3$ coaxial Ge(Li) detector was used. The over-all accuracy of energy determination of reaction $\gamma$ rays in this report was ±1.0 keV or so.

The targets were metallic foils of enriched isotopes of $^{204}$Pb, $^{206}$Pb, $^{207}$Pb, and $^{208}$Pb. The thickness was about 20 mg/cm$^2$. Of these the enrichment of the $^{204}$Pb target was so poor that $\gamma$ rays resulting from the other isotopes were observed. Only the $^{204}$Pb target had an 800-$\mu$g/cm$^2$-thick Mylar backing.

The $\gamma$-ray signal from the Ge(Li) detector passing

* Work performed under the auspices of the U.S. Atomic Energy Commission.

[1] T. Yamazaki and G. T. Ewan, Phys. Letters **24B**, 278 (1967).
[2] T. Yamazaki and G. T. Ewan, Nucl. Instr. Methods **62**, 101 (1968).
[3] T. Yamazaki, G. T. Ewan, and S. G. Prussin, Phys. Rev. Letters **20**, 1376 (1968).
[4] T. Yamazaki and G. T. Ewan, Nucl. Phys. **A134**, 81 (1969).
[5] T. Yamazaki, in *International School of Physics "Enrico Fermi" Course 40*, edited by M. Jean and R. A. Ricci (Academic Press Inc., New York, 1969) p. 791.
[6] W. J. Treytl, E. K. Hyde, and T. Yamazaki, Nucl. Phys. **A117**, 481 (1968).
[7] T. Yamazaki and E. Matthias, Phys. Rev. **175**, 1476 (1968).
[8] C. K. Hargrove and W. M. Martin, Can. J. Phys. **40**, 964 (1962).
[9] I. Perlman, F. Asaro. A. Ghiorso, A. Larsh, and R. Latimer, Phys. Rev. **127**, 917 (1962).

through a fast preamplifier was split into one signal for pulse-height (energy) analysis and another for time analysis. The fast signal was used to generate the start signal for a time-to-amplitude converter, and the rf signal from the cyclotron oscillator was used to generate the stop signal, thus yielding a time pulse height corresponding to the time between the $\gamma$ ray and the cyclotron burst. Figure 1 shows a prompt time distribution with the 30-cm$^3$ Ge(Li) detector (511 keV), referred to a NaI(Tl) signal in a coincidence mode. A time spread of 6.3-nsec full width at half-maximum (FWHM) was obtained and the half-slope for the Ge(Li) delay was about 1.8 nsec. For lower $\gamma$-ray energies the time resolution was worse. In a few cases, planar-type Ge(Li) detectors were employed, which showed better time resolution.

The energy and time signals were fed into a 4096-channel two-dimensional pulse-height analyzer. For survey runs 1024 channels were used for energy spectra routed by four time segments (prompt, delayed 1, 2, and 3). Such runs at once revealed delayed $\gamma$ rays and gave rough estimates of half-lives. For a precise determination of half-lives, more time channels in a two-parameter mode were used.

The time intervals of beam bursts were 182 nsec for 24-MeV $\alpha$, 163 nsec for 30-MeV $\alpha$, 142 nsec for 40-MeV $\alpha$, and 127 nsec for 50-MeV $\alpha$. Delayed $\gamma$ rays of half-lives longer than 200 nsec were easily identified but the half-lives could not be determined within these too-short time intervals.

### B. Analysis of the Experimental Data

The predominant reactions were of ($\alpha$, $xn$) type and typically ($\alpha$, $2n$) with 30-MeV $\alpha$'s, ($\alpha$, $3n$) with 40-MeV $\alpha$'s and ($\alpha$, $4n$) with 50-MeV $\alpha$'s. At 24 MeV the ($\alpha$, $n$) cross section is comparable to the ($\alpha$, $2n$) cross section, and $\gamma$ rays from the ($\alpha$, $n$) reaction are relatively pronounced. Other reactions such as ($\alpha$, $pxn$) are assumed to be weak for these heavy nuclei. A reasonable isotope identification was obtained as shown in each figure by cross checking various reactions.

In general, a high-spin isomeric state proceeds to the ground state via two or more $\gamma$ transitions. The isomeric transition and subsequent ones appear in a delayed energy spectrum, but the subsequent transitions have prompt components because they are populated as well through states other than the isomeric state. Most of the delayed $\gamma$ rays turned out to be such prompt transitions that are preceded by an isomeric state. Isomeric transitions themselves are often missed because of their low energies and high conversion rates.

The relative intensities of prompt components of transitions following the decay of an isomeric state served as a powerful clue to determine the order of the transitions, since a lower-lying level receives more prompt population than a higher-lying level.

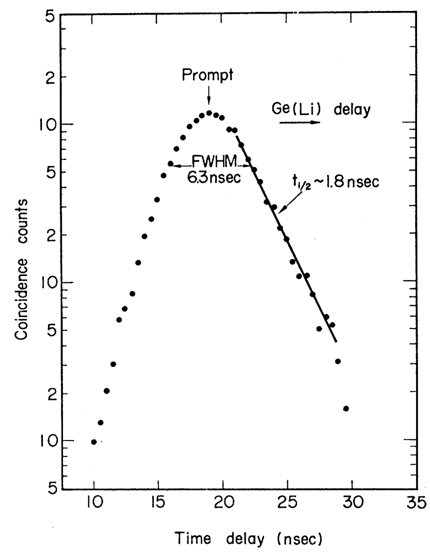


FIG. 1. Prompt timing curve with a 30-cm$^3$ coaxial Ge(Li) detector (511 keV) examined with reference to a NaI(Tl) detector (511 keV) in coincidence.

In case the ground state of a product nucleus is short-lived ($\lesssim$1 h), $\gamma$ rays following the electron-capture (EC) decay or $\alpha$ decay of this nucleus may also be present in delayed spectra. Such $\gamma$ rays should have no prompt component. Therefore, the identification of weak delayed $\gamma$ rays without prompt component were carefully examined by considering the known decay schemes[10] of reaction products.

## III. LEVEL SCHEMES

The level scheme of $^{210}$Po is the most basic as this nucleus consists of 82+2 protons and 126 closed-shell neutrons. Therefore, we shall start with this nucleus and proceed to lighter ones. The level structure of each Po isotope may be compared with the two-proton levels appearing in $^{210}$Po and with the neutron levels appearing in the corresponding Pb isotope of the same neutron number. Such a comparison was made for $^{208}$Po in Ref. 6 and for $^{209}$Po in Ref. 7 and showed that higher-spin states correspond energetically either to proton states or to neutron states. This fact is due to the limited number of configurations for high-spin states. In the following discussion, we shall attempt to make such a comparison using known level structures of Pb isotopes.

### A. $^{210}$Po

Figure 2 shows prompt and delayed $\gamma$-ray spectra from the $^{208}$Pb+30-MeV $\alpha$ reaction, which exhibits $\gamma$

[10] C. M. Lederer, J. M. Hollander, and I. Perlman, *Table of Isotopes* (John Wiley & Sons, Inc., New York, 1967), 6th ed.

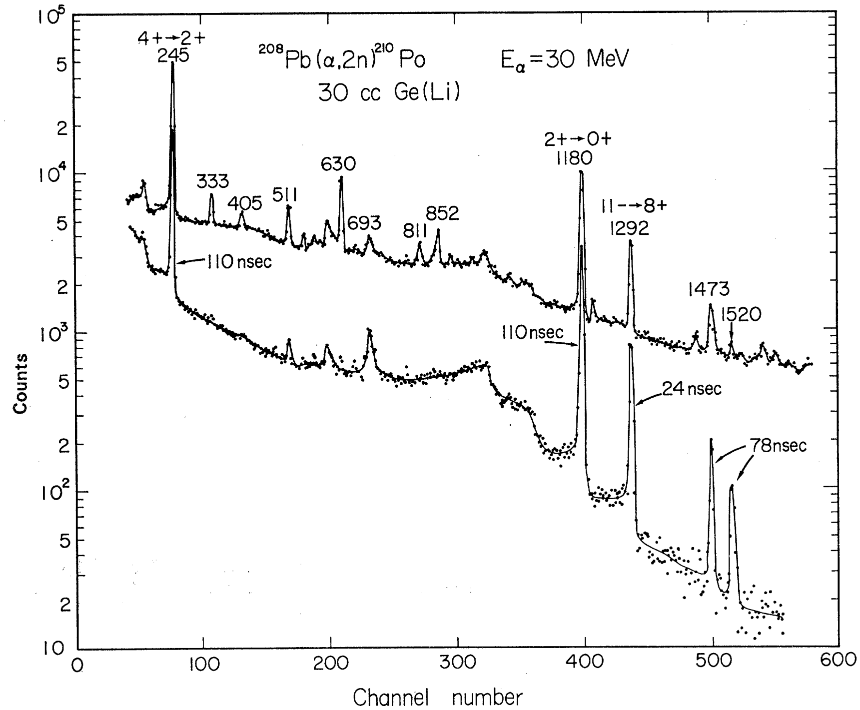


FIG. 2. Prompt and delayed $\gamma$-ray spectra from the $^{208}Pb$+30-MeV $\alpha$ reaction. Almost all peaks result from the $^{208}Pb(\alpha, 2n)^{210}Po$ reaction.

rays assigned to $^{210}Po$. A proposed level scheme is presented in Fig. 3. The 2+, 4+, and 6+ members of the $h_{9/2}{}^2$ configuration had been known from the decay of $^{210}At$,[11,12] and the half-lives of the 4+ and 6+ states were determined by Funk *et al.*[11] Yamazaki and Ewan,[1] observing that the 1180-keV (2+→0+) and 245-keV (4+→2+) transitions follow a half-life of about 150 nsec, which is much longer than the half-life of the 6+ state of 38 nsec, concluded the presence of the 8+ member above the 6+ state. The 8+→6+ transition itself was missing because of its low energy (being highly converted), but the 150-nsec half-life was assigned to this 8+ state. Recently, Ishihara *et al.*[13] measured the time distribution of the 245-keV $\gamma$ ray in a 1.17-$\mu$sec time interval of beam bursts and obtained a revised half-life of 110 nsec. Their time distribution showed a striking growth effect because of the population of the 8+ state through a 24-nsec state which had also been identified by Yamazaki and Ewan.[1]

The 1292-keV $\gamma$ ray followed a half-life of 24 nsec without prompt component, and was interpreted as corresponding to a transition into the 8+ state. This transition was assigned as $E3$ on the basis of its half-life and an 11− spin was given to the 24-nsec state.[1] This interpretation is supported by theoretical considerations since an 11− state is predicted to be the lowest member of the $h_{9/2}i_{13/2}$ configuration.[14] This point including the transition probability will be discussed in Sec. IV.

In addition to the above-mentioned delayed $\gamma$ rays, two delayed lines of the 78-nsec half-life appeared at

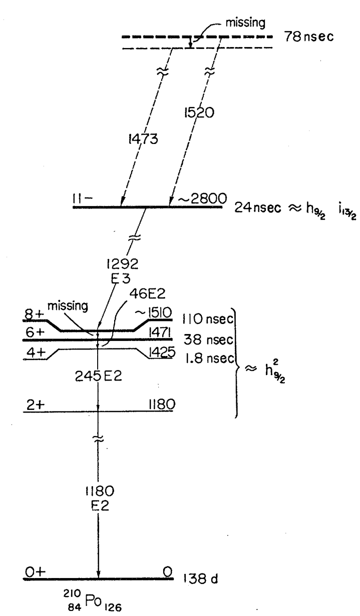


FIG. 3. Proposed level scheme of $^{210}Po$. The placement of the highest two levels is very tentative.

[11] E. G. Funk, Jr., H. J. Prask, F. Schima, J. McNulty, and J. W. Mihelich, Phys. Rev. **129**, 757 (1962).

[12] S. G. Prussin and J. M. Hollander, Nucl. Phys. **A110**, 176 (1968).

[13] M. Ishihara, Y. Gono, K. Ishii, M. Sakai, and T. Yamazaki, Phys. Rev. Letters **21**, 1814 (1968).

[14] Y. E. Kim and J. O. Rasmussen, Nucl. Phys. **47**, 184 (1963); **61**, 173 (1965).

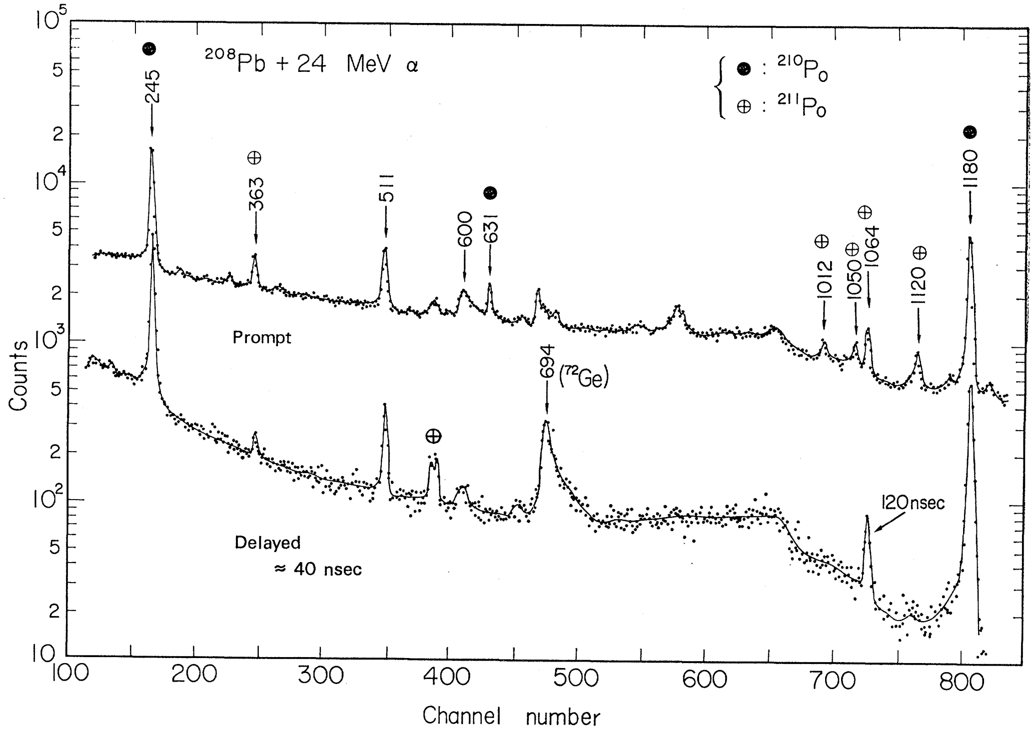


FIG. 4. Prompt and delayed $\gamma$-ray spectra from the $^{208}$Pb+24-MeV $\alpha$ reaction. Predominant reactions are $^{208}$Pb($\alpha$, $2n$)$^{210}$Po and ($\alpha$, $n$)$^{211}$Po, but only very small amount of $^{211}$Po $\gamma$ rays are seen presumably due to the presence of the $\alpha$-decaying isomer.

1473 and 1520 keV, of which the 1473-keV line has a prompt component. Although the energy difference of 47 keV agrees with the 6+→4+ level spacing, a placement of these transitions ending at the 4+ and 6+ levels would conflict seriously with the fact mentioned. An alternative placement as shown in Fig. 3 is likely but only tentative. The two transitions may

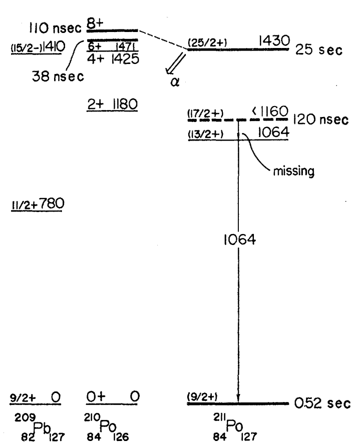


FIG. 5. Proposed level scheme of $^{211}$Po. The 1064-keV $\gamma$ ray is presumably preceded by a 120-nsec isomeric state, whose population is, however, suppressed due to the trap of the 25-sec $\alpha$-decaying isomer. The level scheme is compared with those of $^{210}$Po and of the corresponding $^{209}$Pb.

end either at the 8+ level or at the 11− level, but the latter is preferred because (a) the time distribution of the 1292-keV $\gamma$ ray seems to have a longer component and (b) the two transitions disappear at 24-MeV incident energy, indicating that higher spins are associated with them. This tentative placement is open to further investigation. In any case, the nature of the proposed isomeric state is unknown and seems to be rather mysterious.

### B. $^{211}$Po

The spectra from the $^{208}$Pb+24-MeV $\alpha$ reaction, shown in Fig. 4, exhibit a delayed 1064-keV transition assigned to $^{211}$Po. This energy agrees with that of the 13/2+→5/2− transition in $^{207}$Pb which could be populated by the $\alpha$ decay of $^{211}$Po. However, this assignment is rejected because of the presence of a prompt component and its half-life of 120±40 nsec. Since there is no delayed $\gamma$ ray of the same half-life and intensity, this transition is readily placed between a 1064-keV level and the ground state. The missing isomeric transition, which should have an energy lower than 100 keV, is placed as shown in Fig. 5.

The 25-sec $\alpha$-decaying isomeric state observed by Perlman *et al.*[9] is located at 1430 keV. This excitation energy is approximately equal to the excitation energy of the 8+ state in $^{210}$Po. A 25/2+ spin was assigned to this state, which is the highest spin available with the

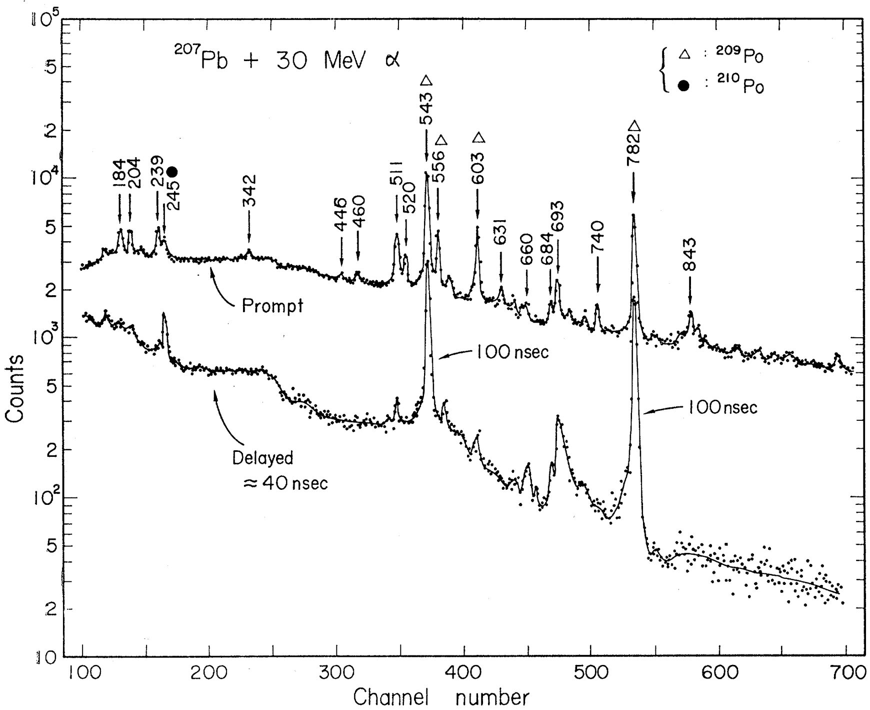


FIG. 6. Prompt and delayed $\gamma$-ray spectra from the $^{207}$Pb+30-MeV $\alpha$ reaction. The $^{207}$Pb$(\alpha, 2n)^{209}$Po reaction is predominant.

$h_{9/2}{}^2(p)g_{9/2}(n)$ configuration. The 21/2+ member of this configuration should lie somewhere around the 25/2+ state, but the fact that the 25/2+ state is long-lived indicates that it is located above the 25/2+ state, thus yielding a large spin gap.

It is to be noted that the $\gamma$-ray yield of $^{211}$Po from the $^{208}$Pb+24-MeV $\alpha$ reaction is remarkably low. It was observed that at $E_\alpha = 24$ MeV the 1180- or 245-keV $\gamma$ ray belonging to the $^{207}$Pb$(\alpha, n)^{210}$Po reaction has nearly the same intensity as the 545- or 782-keV $\gamma$ ray belonging to the $^{207}$Pb$(\alpha, 2n)^{209}$Po reaction. On the other hand, the 1064-keV $\gamma$ ray from the $^{208}$Pb$(\alpha, n)^{211}$Po reaction at $E_\alpha = 24$ MeV is about 10% as intense as the 1180-keV $\gamma$ ray from the $^{208}$Pb$(\alpha, 2n)^{210}$Po reaction (see Fig. 4). This fact is readily related to the presence of the $\alpha$-decaying isomeric state of spin, 25/2+[9], which is supposed to receive a considerable part of the total $\gamma$ decay flow from the continuum region.

### C. $^{209}$Po

Figure 6 shows the $\gamma$-ray spectra from the $^{207}$Pb+30-MeV $\alpha$ reaction. There are two prominent transitions of 545 and 782 keV in the delayed spectrum. The half-life was determined to be 100 nsec, but the isomeric transition was missing. Based on the prompt intensities, Yamazaki and Matthias[7] placed them in cascade as shown in Fig. 7. They also measured the angular distributions of these $\gamma$ rays and established the spin sequence $\frac{9}{2}- \rightarrow \frac{5}{2}- \rightarrow \frac{1}{2}-$. This level scheme is quite different from that obtained by Stoner[15] from the decay of $^{209}$At. Guided by the correspondence with the $^{210}$Po levels and the $p_{1/2}$ ground state of $^{207}$Pb, we may expect two isomeric transitions as suggested in Fig. 7, but this point has not been cleared up experimentally. Yamazaki and Matthias[7] determined the $g$ factor of this isomeric state, and concluded that this state should be a three-particle state with a configuration $[(h_{9/2}{}^2(p))8+$ or $6+, p_{1/2}(n)]17/2-$ or $13/2-$.

### D. $^{208}$Po

The $\gamma$-ray spectrum from the $^{206}$Pb+30-MeV $\alpha$ reaction is shown in Fig. 8. The $^{208}$Po isotope was

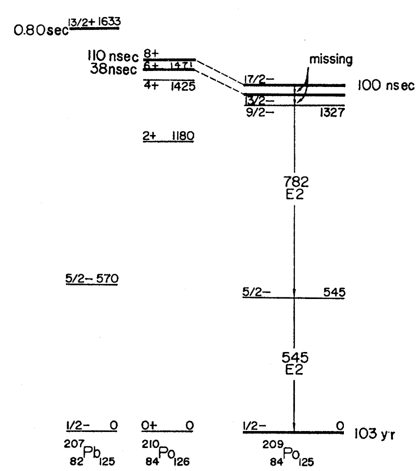


FIG. 7. Level scheme of $^{209}$Po proposed in Ref. 7. This level scheme is compared with those of $^{210}$Po and of the corresponding $^{207}$Pb.

[15] A. W. Stoner (Ph.D. thesis), University of California Report No. UCRL-3471, 1956 (unpublished).

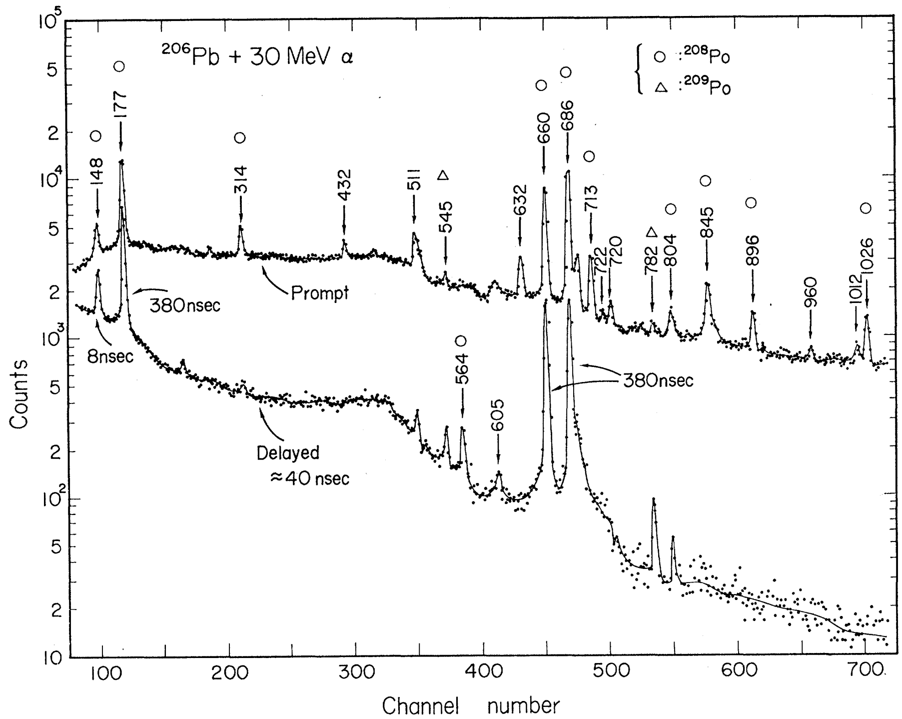


FIG. 8. Prompt and delayed γ-ray spectra from the $^{206}$Pb+30-MeV α reaction. The $^{206}$Pb(α, 2n)$^{208}$Po reaction is predominant.

studied extensively by Treytl, Hyde, and Yamazaki[6] from the $^{208}$At decay as well as from the $^{208}$Pb(α, 4n)$^{208}$Po and $^{209}$Bi(p, 2n)$^{208}$Po reactions. They placed the three delayed transitions of 176, 660, and 685 keV with 380-nsec half-life in cascade by a coincidence experiment. Furthermore, measurements of the angular distribution and the conversion coefficients established the 6+→4+→2+→0+ sequence, as shown in Fig. 9. The half-life of the 6+ state was determined to be 4 nsec with the delayed coincidence method in the $^{208}$At decay. The missing transition was searched for with a Si(Li) detector in the $^{208}$At decay and the upper limit of the transition energy was found to be about 10 keV. The 147-keV transition, which was found to have an 8-nsec half-life,[1,2] is not placed in the level scheme of Fig. 9.

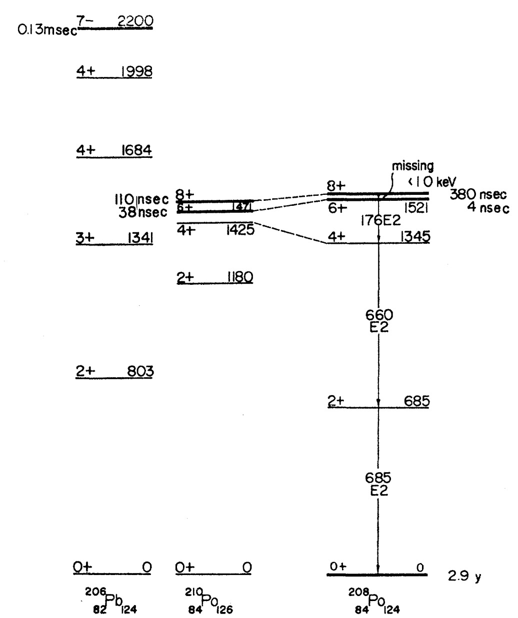


FIG. 9. Level scheme of $^{208}$Po, proposed in Ref. 6. This level scheme is compared with those of $^{210}$Po and of the corresponding $^{206}$Pb.

## E. $^{207}$Po

The γ-ray spectrum from the $^{204}$Pb+24-MeV α reaction is shown in Fig. 10. Because of the poor enrichment of this isotope there appear to be many peaks resulting from other isotopes, but careful cross checks led to reasonable identification of peaks. Two isomeric states were identified by Hargrove and Martin[8] in the $^{209}$Bi(p, 3n)$^{207}$Po reaction. They measured delayed γ rays with a scintillation spectrometer and obtained an unambiguous level scheme based on the lifetime measurements and multipolarity assignments from x-ray yields associated with the isomeric transitions. Figure 11 reproduces their level scheme with the more precise energy values obtained here. Figure 10 exhibits weak prompt and delayed lines, which appear to be long-lived. They have not been placed in the level scheme.

## F. $^{206}$Po

The γ-ray spectrum from the $^{204}$Pb+30-MeV α reaction is shown in Fig. 12. There is no previous information on this nucleus. Just as in the case of $^{208}$Po,

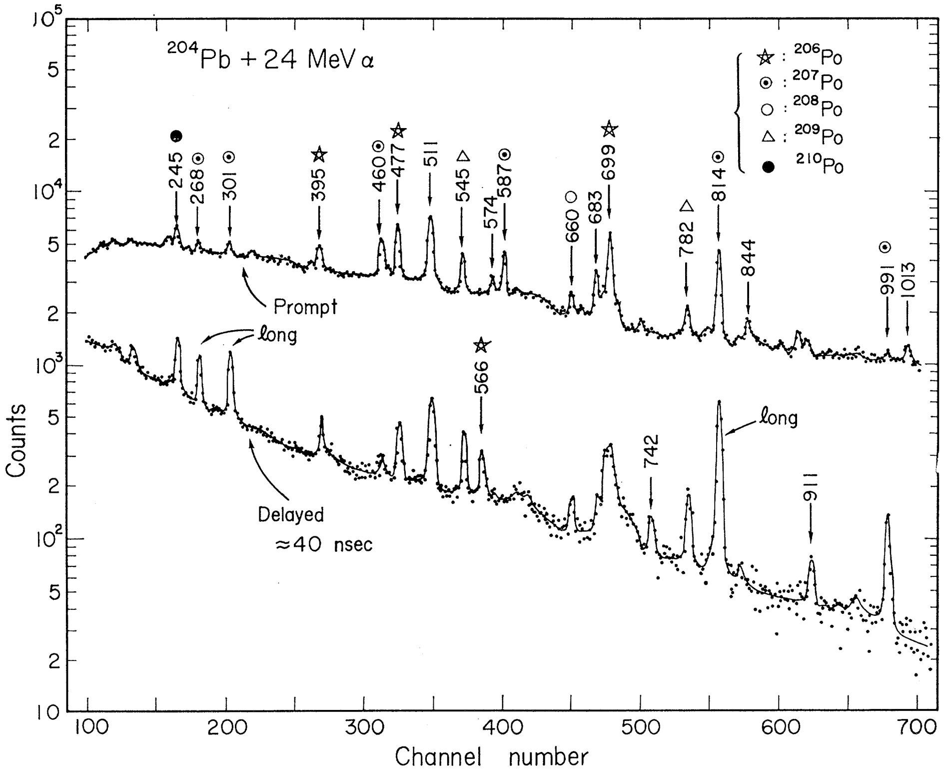


FIG. 10. Prompt and delayed spectra from the $^{204}$Pb+24-MeV α reaction. Predominant are the $^{204}$Pb(α, 2n)$^{206}$Po and $^{204}$Pb(α, n)$^{207}$Po reactions. Impurities in the target yielded other weak lines.

three delayed γ rays of equal intensity were found. These γ rays follow a half-life of 160±40 nsec. The order of these transitions were determined as shown in Fig. 13 from the prompt intensities. No further information is available as to the multipolarities and spins, but it is most likely that the isomeric decay sequence must be just similar to that of $^{208}$Po. The isomeric transition is again missing.

A weak γ ray of 566 keV was found to decay with a 100-nsec half-life. Since it has no prompt component, it is an isomeric transition. If it is located up above feeding the 8+ isomeric state, we obtain an isomeric state around 2160 keV. There should be a 9− state in $^{206}$Po corresponding to the 9− state in $^{204}$Pb. The 9− state in $^{206}$Po, if it exists, proceeds to the 8+ state via $E1$, but this $E1$ transition must be highly hindered, since to the zeroth approximation the 9− state is a two-neutron state and the 8+ state is a two-proton state. The isomeric state we postulate at 2160 keV might be such a state. This point will be discussed in Sec. IV.

### G. $^{205}$Po

The γ-ray spectrum from the $^{204}$Pb+40-MeV α reaction is shown in Fig. 14. The 0.6-msec $^{205m}$Po was found by Link,[16] and studied by Hargrove and Martin[8] in the $^{209}$Bi(p, 5n)$^{205}$Po reaction. They found two delayed γ rays of 707 and 160 keV. From the relative intensities of these γ rays and the K x rays, they assigned the multipolarity of the 160-keV transition as $M2$. In the present γ-ray spectra, two peaks at 151 and 720 keV appear, which must correspond to those γ rays observed by Hargrove and Martin.[8] The 720-keV γ ray has a prompt component, being consistent with

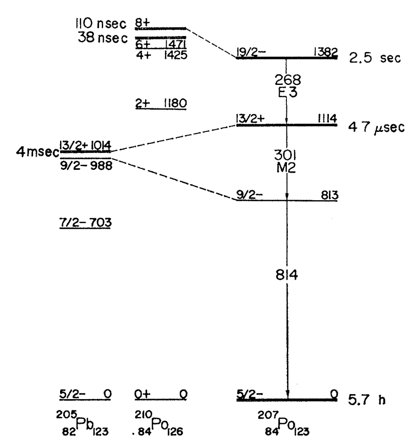


FIG. 11. Level scheme of $^{207}$Po established in Ref. 8. This level scheme is compared with those of $^{210}$Po and of the corresponding $^{205}$Pb.

[16] W. T. Link, Ph.D. thesis, McGill University, 1957 (unpublished).

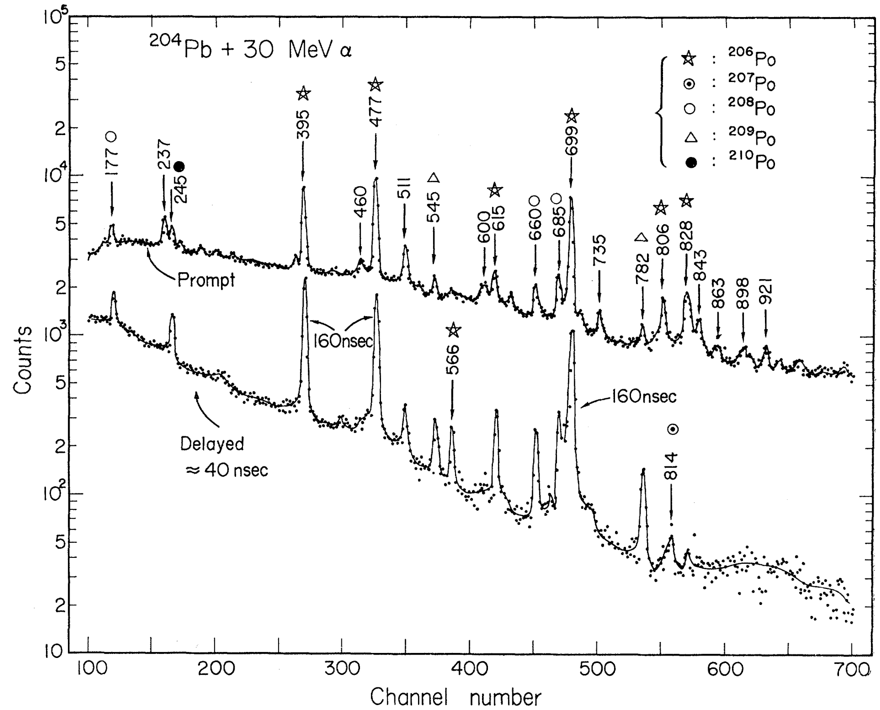


FIG. 12. Prompt and delayed spectra from the $^{204}$Pb+30-MeV $\alpha$ reaction. The $^{204}$Pb($\alpha$, $2n$)$^{206}$Po reaction is predominant.

their level scheme in Fig. 15. The 0.64-msec state may be interpreted as the $i_{13/2}$ neutron state appearing in $^{203}$Pb.

In addition, a long-lived $\gamma$ ray of 873 keV without a prompt component was found. Because its energy equals the sum, 151+720 keV, within the experimental errors the 873-keV transition might be the crossover transition. If so, it should then be the $M4$ transition between the 13/2+ and 5/2− states, but its intensity (about 10% of the 720-keV $\gamma$ ray) leads to a partial half-life of 6 msec for this transition, which contradicts seriously the $M4$ assignment (the Weisskopf estimate is about 10 sec). Therefore, this transition should be located elsewhere. There are some other delayed transitions, but they could not have been incorporated into the present level scheme without much ambiguity.

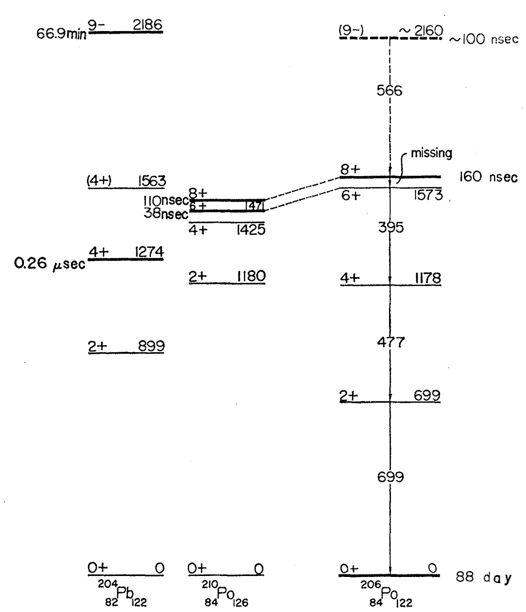


FIG. 13. Proposed level scheme of $^{206}$Po. The highest level is tentative. This level scheme is compared with those of $^{210}$Po and of the corresponding $^{204}$Pb.

## H. $^{204}$Po

The $\gamma$-ray spectrum from the $^{204}$Pb+50-MeV $\alpha$ reaction is shown in Fig. 16. There is no previous information on this nucleus. Just as in the case of $^{208}$Po and $^{206}$Po, three delayed $\gamma$ rays of equal intensity are observed. The three $\gamma$ rays of 427, 517, and 686 keV follow a half-life of 190±20 nsec and the order was determined as shown in Fig. 17 from the prompt intensities. The order of the 517- and 686-keV $\gamma$ rays, however, remains rather ambiguous, since both had nearly the same prompt intensities. A comparison with the level scheme of $^{206}$Po suggests the order shown in Fig. 17. The isomeric transition was not observed. The level structure is quite similar to that of $^{208}$Po and $^{206}$Po.

A weak delayed $\gamma$ ray of 589 keV, which decays with a half-life of about 20 nsec, was also identified. This transition is placed tentatively as feeding the 8+ isomeric state. The same argument presented for the case of $^{206}$Po may be applied here.

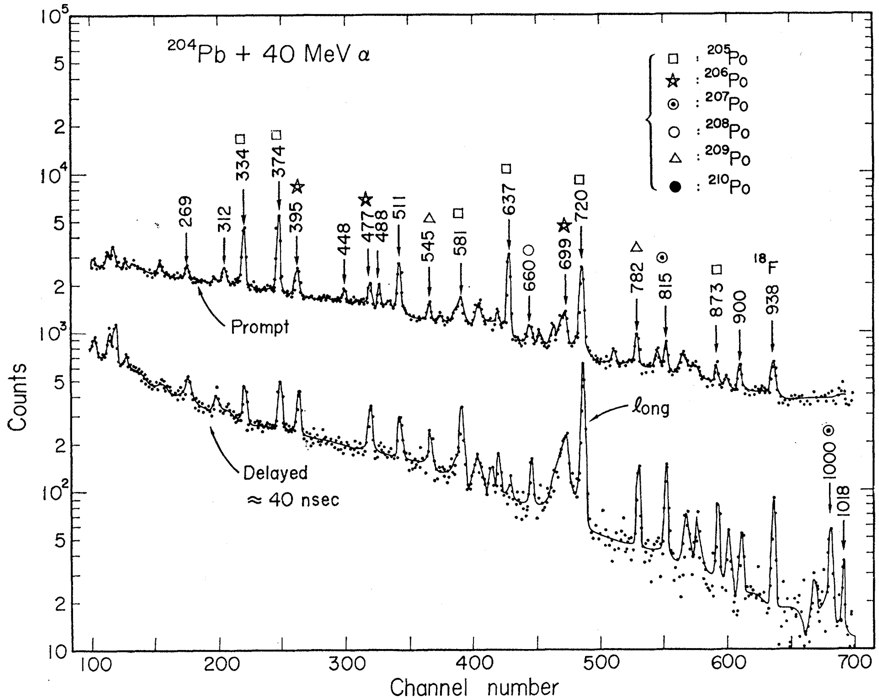


FIG. 14. Prompt and delay spectra from the $^{204}$Pb+40-MeV $\alpha$ reaction. The $^{204}$Pb($\alpha$, $3n$)$^{205}$Po reaction is predominant. Impurities in the target yielded other weak lines.

## IV. DISCUSSION

In this section, we discuss characteristic features revealed in the present experimental study. Excited states of Po isotopes should in principle be described by combining the two-proton excitation appearing in ${}_{84}^{210}\mathrm{Po}_{126}$ with neutron excitations appearing in the corresponding Pb isotopes. Such a detailed shell-model calculation as performed for the case of $^{212}$Po by Glendenning and Harada[17] may be applied, but it is beyond the scope of the present paper. Instead, we attempt to use the weak coupling method, which was applied to $^{208}$Po by Treytl, Hyde, and Yamazaki.[6]

### A. Deduction of $B(E2)$ from Half-Lives

Since the $8+\rightarrow 6+$ isomeric transitions of $E2$ multipolarity are not observed, the transition energies are unknown. It might then seem at first sight impossible to deduce $B(E2)$ values from the half-lives. However, as the internal conversion process predominates in the deexcitation below 100 keV and the conversion emission probability is insensitive to the transition energy $E_\gamma$ (whereas the photon emission probability is proportional to $E_\gamma{}^5$), the half-life $t_{1/2}$ alone leads to $B(E2)$. Explicitly,

$$t_{1/2}(\mathrm{sec}) = X/B(E2)\,(e^2 fm^4),$$

where

$$X = \frac{1}{1.22\times 10^9}\,\frac{0.693}{1+\alpha_{\mathrm{tot}}}\,\frac{1}{[E_\gamma(\mathrm{MeV})]^5}.$$

[17] N. K. Glendenning and K. Harada, Nucl. Phys. **72**, 481 (1965).

The quantity $X$ was calculated with the use of the theoretical $L$ and $M$ subshell conversion coefficients of Hager and Seltzer.[18] We assumed that

$$\alpha_{\mathrm{tot}} = \alpha_L + \alpha_M(1+\tfrac{1}{3}).$$

As seen from Fig. 18, $X$ is nearly a step function of $E_\gamma$. It takes the following approximate values in the two main regions:

$$X = 1.0\times 10^{-5} \quad \text{for} \quad E(K) \gtrsim E_\gamma \gtrsim E(L_2), \qquad \text{(region I)}$$
$$\quad = 4.0\times 10^{-5} \quad \text{for} \quad E(L_3) \gtrsim E_\gamma \gtrsim E(M_2), \qquad \text{(region II)}$$

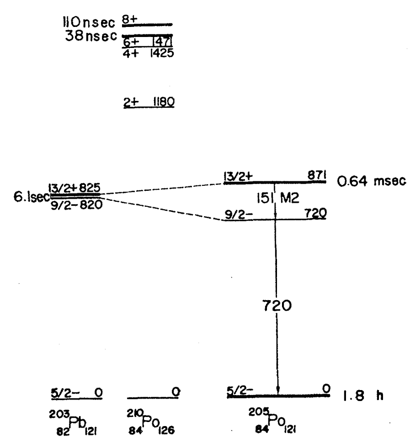


FIG. 15. Level scheme of $^{205}$Po proposed in Ref. 8. This level scheme is compared with those of $^{210}$Po and of the corresponding $^{203}$Pb.

[18] R. S. Hager and E. C. Seltzer, Nucl. Data **A4**, 1 (1968).

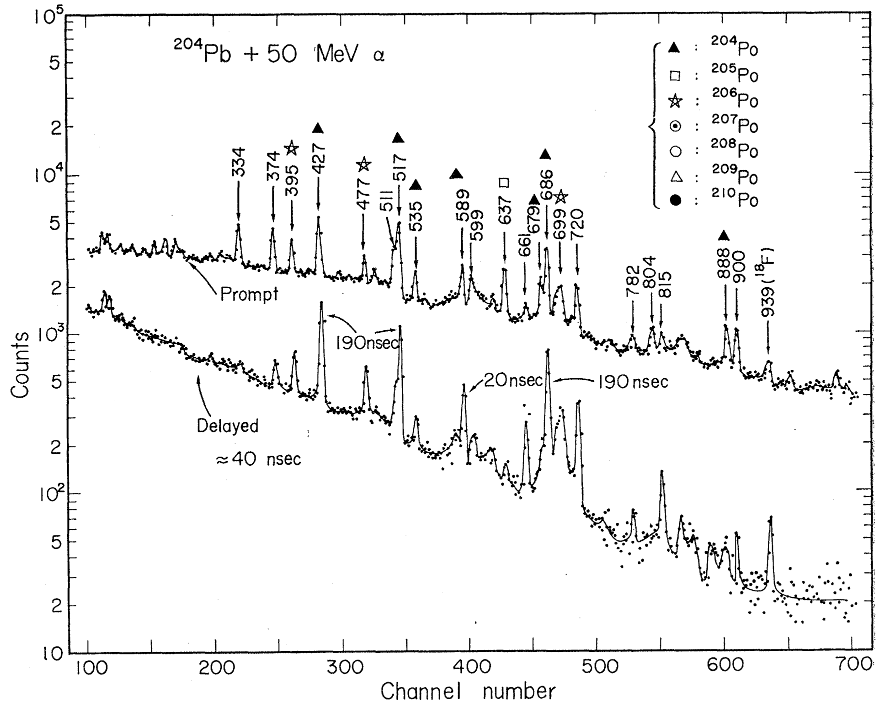


FIG 16. Prompt and delayed spectra from the $^{204}$Pb+50-MeV $\alpha$ reaction. The $^{204}$Pb($\alpha$, $4n$)$^{204}$Po reaction is predominant. Impurities in the target yielded other weak lines.

where $E(L_2)$ stands for the binding energy of an $L_2$-shell electron, etc. Assuming that $E_\gamma$ be either in region I or in region II, we can deduce $B(E2)$ from experimental half-lives, as listed in Table I.

### B. $(h_{9/2}{}^2)J+$ States of $^{210}$Po

According to the shell-model calculation of Kim and Rasmussen,[14] the lowest 0+, 2+, 4+, 6+, and 8+ states are dominated by the $h_{9/2}{}^2$ configuration. The calculated impurity (amplitude of other configurations) is very small. It may be a plausible assumption that the missing level spacing $E(8+\rightarrow 6+)$ is nearly equal to $E(6+\rightarrow 4+)$ or a little less (in region I of Fig. 18). We may then deduce $B(E2, 8+\rightarrow 6+)$ as well as $B(E2, 4+\rightarrow 2+)$ and $B(E2, 6+\rightarrow 4+)$.

A discussion of these $B(E2)$ values was made by Yamazaki[5] and later by Ishihara *et al.*[13] Each $B(E2)$ value within the pure $h_{9/2}{}^2$ configuration is expressed in terms of a radial matrix element as follows:

$$B(E2, (h_{9/2}{}^2)I\rightarrow(h_{9/2}{}^2)I') = S(I\rightarrow I')(4\pi)^{-1} \,|\, \langle h_{9/2} \,|\, e_{\text{eff}} r^2 \,|\, h_{9/2}\rangle \,|^2, \quad (1)$$

where the statistical factor $S(I\rightarrow I')$ is

$$S(I\rightarrow I') = |\, 2(5)^{1/2}[(2I'+1)(2I+1)]^{1/2} \times W(jjI'2; Ij)\langle j\tfrac{1}{2}20 \,|\, j\tfrac{1}{2}\rangle \,|^2.$$

The deduced matrix elements are given in column 5 of Table II. Recently, a precise value of the static quadrupole moment of the $h_{9/2}$ ground state of $^{209}$Bi has been reported[19] as

$$Q(^{209}\text{Bi}) = -0.379 \pm 0.015 \text{ b}.$$

From the relation

$$Q = -\frac{2j-1}{2(j+1)} \langle h_{9/2} \,|\, (e_{\text{eff}}/e) r^2 \,|\, h_{9/2}\rangle,$$

the radial matrix element for $^{209}$Bi is derived as

$$\langle h_{9/2} \,|\, e_{\text{eff}} r^2 \,|\, h_{9/2}\rangle = 52 \pm 2 \; e \text{ fm}^2.$$

Dividing this value by the radial integral of Blomqvist and Wahlborn,[20] one obtains

$$e_{\text{eff}}(^{209}\text{Bi}) = (1.50 \pm 0.06)e.$$

TABLE I. $B(E2, 8+\rightarrow 6+)$ deduced from $t_{1/2}$ when the transition is assumed to be either in region I or in region II (see Fig. 18).

| Isotope | $t_{1/2}(8+\rightarrow 6+)$ (nsec) | $B(E2)$ ($e^2$ fm$^4$) Region I | Region II |
|---|---|---|---|
| $^{210}$Po | 110±10 | 90 | |
| $^{208}$Po | 380±100 | 25 | 100 |
| $^{206}$Po | 160±40 | 63 | 250 |
| $^{204}$Po | 190±20 | 53 | 210 |

[19] G. Eisele, I. Koniordos, G. Müller, and R. Winkler, Phys. Letters **28B**, 256 (1968).
[20] J. Blomqvist and S. Wahlborn, Arkiv Fysik **16**, 545 (1960).

TABLE II. Reduced transition probabilities of the three transitions within the $h_{9/2}^2$ band of $^{210}$Po. The deduced effective charge is compared with that ($e_{eff}=1.50\pm0.06$) of $^{209}$Bi.

| Transition $I_i \to I_f$ | Transition energy (keV) | $t_{1/2}$ (nsec) | $B(E2)$[a] ($e^2$ fm$^4$) | $\langle h_{9/2} \mid e_{eff}r^2 \mid h_{9/2}\rangle$[b] | $e_{eff}(^{210}\text{Po})/e_{eff}(^{209}\text{Bi})$ |
|---|---|---|---|---|---|
| $8+\to6+$ | (35)[c] | $110\pm8$[d] | $87\pm9$ | $60\pm3$ | $1.16\pm0.06$ |
| $6+\to4+$ | 46 | $38\pm5$[e] | $245\pm25$ | $64\pm3$ | $1.22\pm0.06$ |
| $4+\to2+$ | 245 | $1.8\pm0.2$[e] | $285\pm29$ | $57\pm3$ | $1.09\pm0.06$ |

[a] Relative error of about 10% is assigned to these values, supposed to arise from uncertainty in deducing $B(E2)$ from $t_{1/2}$ and from errors in $t_{1/2}$.
[b] Derived from $B(E2)$ with use of Eq. (1) in which the pure configuration of $h_{9/2}^2$ is assumed.
[c] Assumed, as the $\gamma$ ray is missing.
[d] Reference 13.
[e] Reference 11.

The effective charge for $^{210}$Po is compared with this value in column 6 of Table II. It is observed that the effective charge for $^{210}$Po is 10–20% larger than that for $^{209}$Bi.

This increase may be, at least partially, due to the configuration mixing by the outer two particles. Since the spin-flip $E2$ transition such as $f_{7/2}\to h_{9/2}$ is considerably slow, only an admixture of the $h_{9/2}f_{7/2}$ configuration may not be sizable enough. On the other hand, a substantial increase of $B(E2)$ may be expected if the $h_{9/2}f_{5/2}$ state is mixed, although such an admixture is energetically unfavored. Blomqvist[21] evaluated the increase of $B(E2)$ considering the wave functions

$$|I+\rangle = |h_{9/2}^2, I+\rangle + \alpha_I |h_{9/2}f_{7/2}, I+\rangle + \beta_I |h_{9/2}f_{5/2}, I+\rangle.$$

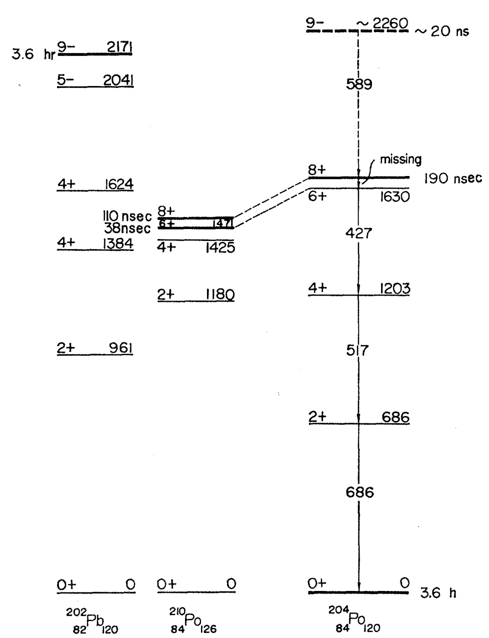


FIG. 17. Proposed level scheme of $^{204}$Po. This level scheme is compared with those of $^{210}$Po and of the corresponding $^{202}$Pb.

[21] J. Blomqvist (private communication); the author is indebted to J. Blomqvist and A. Arima for discussions of this point.

Then the $E2$ transition matrix elements become larger by the following factors:

$$F(8+\to6+) = 1-0.432\alpha_6 t+0.0508\alpha_8 t-2.57\beta_6 t,$$

$$F(6+\to4+) = 1-0.302\alpha_4 t+0.0943\alpha_6 t-1.06\beta_4 t -0.120\beta_6 t,$$

$$F(4+\to2+) = 1-0.216\alpha_2 t+0.134\alpha_4 t-0.403\beta_2 t -0.292\beta_4 t,$$

where

$$t\equiv \langle f \mid r^2 \mid h\rangle / \langle h \mid r^2 \mid h\rangle = -0.47,$$

according to Ref. 20. The mixing amplitudes were calculated with use of the Kuo-Brown matrix elements.[22] Such admixtures, however, turn out to increase the transition amplitude only by 2–3%.

The effective charge $e_{eff}(^{210}\text{Po})$ corrected for the above configuration mixing outside the $^{208}$Pb core is thus

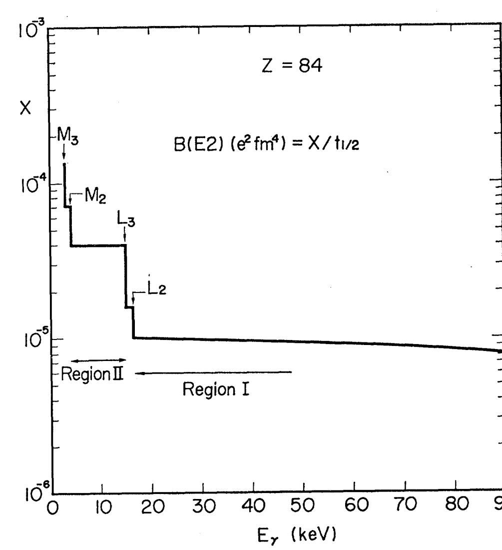


FIG. 18. The quantity $X=t_{1/2}(\text{sec})\times B(E2)$ ($e^2$ fm$^4$) as a function of the transition energy at low energy. The conversion coefficients are taken from Hager and Seltzer (Ref. 18).

[22] T. T. S. Kuo and G. E. Brown, Nucl. Phys. 85, 40 (1966).

still 10% more than $e_{\rm eff}(^{209}\text{Bi})$. This difference might indicate a slight violation of the linearity of the core effective charge, namely, that the $h_{9/2}$ proton feels an increasing core effective charge when another $h_{9/2}$ proton is added. However, it has been pointed out by Arima[23] that a large $h_{9/2}f_{5/2}$ admixture responsible for such a large increase can be caused particularly by the $Q$-$Q$-type correlation between two protons.

Yamazaki[5] reported a preliminary measurement of the $g$ factor of the 8+ state, which was compatible with the $h_{9/2}{}^2$ configuration, if the anomalous $g$ factor of the $h_{9/2}$ state of $^{209}$Bi is persistent in $^{210}$Po.

### C. $(h_{9/2}{}^2)8+$ States of Other Po Isotopes

It is obvious that the isomeric states we observed in the even isotopes are characterized by the $(h_{9/2}{}^2)8+$ configuration. The relevant level systematics is presented in Fig. 19. The positions of the 6+ and 8+ levels remain nearly unchanged, constituting the 8+→6+ $E2$ isomeric transition in each nucleus. The change of the half-lives is related to both $E(8+\rightarrow 6+)$ and $B(E2, 8+\rightarrow 6+)$. The longest half-life (380 nsec) is observed in $^{208}$Po. This fact should be due either to a very small $B(E2)$ or to a very small level spacing (region II in Fig. 18). Treytl, Hyde, and Yamazaki[6] searched for the missing conversion electrons in the $^{208}$At decay and concluded that the transition energy is actually less than 10 keV (region II).

The 8+→6+ level spacing and B$(E2, 8+\rightarrow 6+)$ were studied theoretically by Treytl, Hyde, and Yamazaki.[6] They evaluated the effect of the $E2$ core vibration on the $(h_{9/2}{}^2)J+$ states with the weak coupling method. We now apply their procedure to the other isotopes. In this procedure, the effect of neutron excitation is replaced by a quadrupole vibration. The

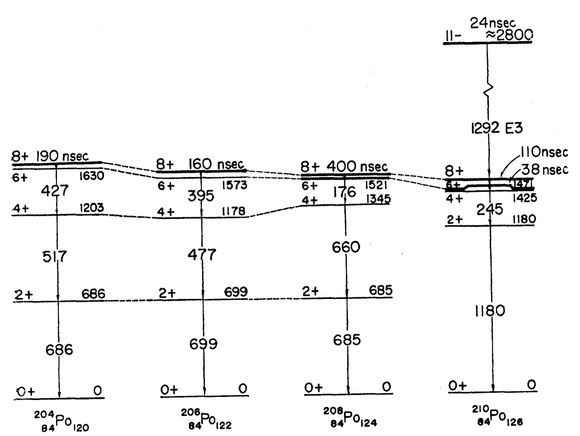


FIG. 19. Isomer systematics of even Po isotopes. These 8+ isomeric states are characterized by the $h_{9/2}{}^2$ proton configuration.

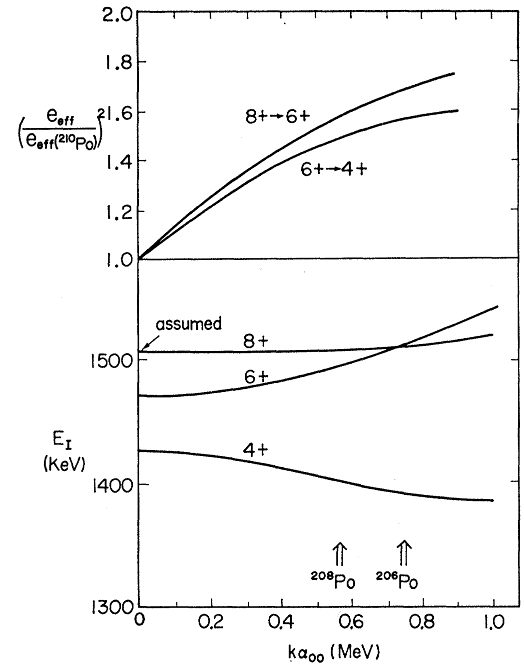


FIG. 20. Calculated energies and enhancement factors of the $h_{9/2}{}^2$ states which are weakly coupled with the $E2$ vibration of the Pb core.

interaction Hamiltonian is thus

$$H_{\rm int}=-k(\hbar\omega/2C)^{1/2}\sum_{\mu}\{b_\mu+(-)^\mu b_{-\mu}{}^+\}\{Y_{2\mu}(\theta_1,\phi_1)+Y_{2\mu}(\theta_2,\phi_2)\},$$

where the coupling constant $k$ has a magnitude of 40 MeV according to Bohr and Mottelson.[24]

The vibrational amplitude $\alpha_{00}$ is given in terms of $B(E2)$ of the corresponding core $^{A-2}$Pb as follows:

$$\alpha_{00}\equiv(\hbar\omega/2C)^{1/2}=\frac{[B(E2, 2+\rightarrow 0+, {}^{A-2}\text{Pb})]^{1/2}}{(3/4\pi)ZeR_0{}^2}.$$

In the following qualitative discussions we leave $k\alpha_{00}$ as a free parameter which changes from nucleus to nucleus. To the lowest order of the coupling of the two-particle state with vibration, the perturbed states are given by

$$\begin{aligned}|I\rangle=a_1{}^I|(h_{9/2}{}^2)I,(0\hbar\omega)0;I\rangle\\+a_2{}^I|(h_{9/2}{}^2)I-2,(1\hbar\omega)2;I\rangle\\+a_3{}^I|(h_{9/2}{}^2)I,(1\hbar\omega)2;I\rangle\\+a_4{}^I|(h_{9/2}{}^2)I+2,(1\hbar\omega)2;I\rangle\end{aligned}$$

and

$$\begin{aligned}B(E2, I\rightarrow I-2, {}^A\text{Po})&=|a_1{}^{I-2}a_1{}^I[B(E2, I\rightarrow I-2, {}^{210}\text{Po})]^{1/2}\\&-\{a_1{}^{I-2}a_2{}^I+[(2I-3)/(2I+1)]^{1/2}a_1{}^Ia_4{}^{I-2}\}\\&\times[B(E2, 2+\rightarrow 0+, {}^{A-2}\text{Pb})]^{1/2}|^2.\end{aligned}$$

[23] A. Arima (private communication).

[24] A. Bohr and B. R. Mottelson, Kgl. Danske Videnskab. Selskab, Mat.-Fys. Medd. 27, No. 16 (1953).

The energies and the amplitudes $a_i^I$ were obtained by diagonalizing the interaction Hamiltonian. Detailed expressions are given in Ref. 6.

The coupling of vibration always increases $B(E2, I\rightarrow I')$, and this increase is represented by an effective charge which is larger than that for $^{210}$Po. The calculated energies and the enhancement factor $[e_{\text{eff}}/e_{\text{eff}}(^{210}\text{Po})]^2$ are plotted in Fig. 20 as functions of $k\alpha_{00}$. Such an expected enhancement of $B(E2)$ is observed in the 176-keV $6+\rightarrow 4+$ transition of $^{208}$Po,[6] where the enhancement factor is 1.8.

While the calculated $B(E2)$ increases only by 50%, the calculated $8+\rightarrow 6+$ energy decreases rapidly, and with larger $k\alpha_{00}$ the level order would be reversed. This calculation implies that it may be mainly due to $E(8+\rightarrow 6+)$ that $t_{1/2}(8+\rightarrow 6+)$ changes from nucleus to nucleus. The fact that the experimental half-lives of $^{204}$Po, $^{206}$Po, and $^{208}$Po are all longer than that of $^{210}$Po implies that the $8+\rightarrow 6+$ energies of the former isotopes may be considerably less than that of $^{210}$Po (in between region I and II or in region II of Fig. 18).

Experimental values of $B(E2, 2+\rightarrow 0+, \text{Pb})$ are known[25] for $^{206}$Pb and $^{204}$Pb. The $k\alpha_{00}$ values for $^{208}$Po and $^{206}$Po with a fixed $k$ value of 40 MeV[24] are indicated in Fig. 20. This calculation predicts a longer half-life for $^{206}$Po, but the observed one is shorter. On the basis of the present data, we shall not go into further discussion.

### D. 11− State of $^{210}$Po

The 24-nsec state of $^{210}$Po must be the 11− state, which is predicted as the lowest member of the $h_{9/2}i_{13/2}$ configuration.[14] Yamazaki[5] reported a preliminary measurement of the $g$ factor of this state, which is compatible with the $(h_{9/2}i_{13/2})11-$ configuration.

The $E3$ transition probability is easily estimated by assuming the shell-model configurations.[26] In the present case,

$$B(E3, 11-\rightarrow 8+)_{\text{shell model}}=146\ e^2\ \text{fm}^6.$$

On the other hand,

$$B(E3, 11-\rightarrow 8+)_{\text{expt}}=8500e^2\ \text{fm}^6,$$

which is considerably larger than the shell-model estimate. This fact implies a large contribution of the octupole vibration appearing in the $^{208}$Pb core ($\hbar\omega_3=$ 2614 keV). Assuming wave functions of the form

$$|\,8+\rangle=(1-\alpha_8^2)^{1/2}\,|\,(h_{9/2}^2)8+\rangle +\alpha_8\,|\,3-, (h_{9/2}i_{13/2})11-; 8+\rangle,$$

$$|\,11-\rangle=(1-\alpha_{11}^2)^{1/2}\,|\,(h_{9/2}i_{13/2})11-\rangle +\alpha_{11}\,|\,3-, (h_{9/2}^2)8+; 11-\rangle,$$

one obtains

$$B(E3)=\left|(146)^{1/2}\pm\alpha_{11}\frac{2\hbar\omega_3}{\hbar\omega_3+E(11-)-E(8+)}\times[B(E3, 3-\rightarrow 0+, {}^{208}\text{Pb})]^{1/2}\right|^2 e^2\ \text{fm}^6,$$

which yields

$$\alpha_{11}^2\approx 0.05,$$

if the plus sign is chosen.

This situation is equivalent to the case in $^{209}$Bi. The $(d, d')$ experiment on $^{209}$Bi by Diamond[27] indicated that the lowest 13/2+ excited state involves a similar admixture of the octupole state coupled to the 9/2− ground state.

It is to be noted that no isomeric state of the $(h_{9/2}i_{13/2})11-$ configuration is found in other Po isotopes. This fact may be due to the presence of other states (for instance, 9− state) below the 11− state in question.

### E. Possible 9− States in $^{206}$Po and $^{204}$Po

As discussed in Sec. III, 9− isomeric levels are tentatively assigned to $^{206}$Po and $^{204}$Po from the correspondence with the known Pb excitation. The delayed transitions are then interpreted as $E1$ transitions between the 9− and 8+ levels. The hindrance factors are $7.4\times 10^{-9}$($^{206}$Po) and $3.2\times 10^{-8}$($^{204}$Po). These large hindrances may be ascribed to the nonoverlapping of the wave functions, if the 9− state is mainly the neutron state of configuration $f_{5/2}i_{13/2}$ while the 8+ state is mainly the proton state of $h_{9/2}^2$.

### F. Odd Isotopes

The $\alpha$-decaying isomeric state of $^{211}$Po is supposed to be the 25/2+ state in which the $g_{9/2}$ proton is coupled stretchwise to the 8+ state of $^{210}$Po.[9] The large spin gap is explained by the shell-model calculation of Auerbach and Talmi.[28] The tentative level scheme shown in Fig. 5 does not, however, seem to correspond to the predicted levels.

The 100-nsec isomeric state of $^{209}$Po was interpreted by Yamazaki and Matthias[7] as the 17/2− state in which the $p_{1/2}$ neutron hole is coupled stretchwise to the 8+ state of $^{210}$Po. This interpretation is supported by the fact that the spin of the ground state of $^{208}$Bi with a predominant configuration $p_{1/2}^{-1}(n)h_{9/2}(p)$ seems to be 5+ rather than 4+.[10] The measured $g$ factor and $B(E2)$ are compatible with this interpretation, as discussed in Ref. 7. It was shown that the following

[25] P. H. Stelson and L. Grodzins, Nucl. Data **A1**, 21 (1965).
[26] The author is indebted to B. R. Mottelson and J. Blomqvist for discussions of this point. See also, B. R. Mottelson, J. Phys. Soc. Japan Suppl. **24**, 87 (1968).
[27] R. M. Diamond (private communication); see also Ref. 26.
[28] N. Auerbach and I. Talmi, Phys. Letters **10**, 297 (1964).

identities hold quite well:

$$g[(h_{9/2}{}^2)J_p, j_n=\tfrac{1}{2}; I=J_p+\tfrac{1}{2}, {}^{209}\text{Po}]$$
$$=[(2I-1)/2I]g(h_{9/2}, {}^{209}\text{Bi})+(1/2I)g(p_{1/2}, {}^{207}\text{Pb}),$$
$$B[E2, (h_{9/2}{}^2)J_p, j_n; I=J_p+j_n \rightarrow (h_{9/2}{}^2)J_p', j_n; I'=J_p'+j_n]$$
$$=B[E2, (h_{9/2}{}^2)J_p \rightarrow (h_{9/2}{}^2)J_p'].$$

The level structure of $^{207}$Po is rather different from that of $^{209}$Po. In the $^{207}$Po nucleus the ground state is the $f_{5/2}$ neutron hole state and the $i_{13/2}$ neutron hole state lies only at 1 MeV. The 47-$\mu$sec state may be the $i_{13/2}$ state. The highest spin of the $f_{5/2}$ hole coupled to the 8+ state of $^{210}$Po is 21/2−, but the $E3$ character of the 2.5-sec 268-keV transition[8] limits the spin-parity of this long-lived isomeric state to 19/2, which is $2J_p+j_n-1$. This fact is consistent with the spin-parity 6+ of the $^{206}$Bi ground state in which the $f_{7/2}{}^{-1}(n)$ and $h_{9/2}(p)$ orbits are coupled to $I=j_p+j_n-1$ in accordance with the Brennan-Bernstein rule.[29]

In $^{205}$Po, only the $i_{13/2}$ isomeric state is established. The experiment is not conclusive as to the presence of another isomeric state involving the $(h_{9/2}{}^2)8+$ state of $^{210}$Po.

[29] M. H. Brennan and A. H. Bernstein, Phys. Rev. **120**, 927 (1960).

### G. Concluding Remarks

The present survey work has revealed a systematic presence of isomeric states in even and odd Po isotopes which involve the $(h_{9/2}{}^2)8+$ configuration. The present study has shown quite complex structures of isomerisms in these isotopes, and much should thus be done in the future, such as measurements of conversion electrons, decay measurements in expanded time scales and coincidence studies.

### ACKNOWLEDGMENTS

The author would like to thank Dr. J. M. Hollander for his continuous encouragement and Dr. C. M. Lederer, Dr. S. G. Prussin, and Dr. J. M. Jaklevic for their help during this work. He is grateful to Dr. J. Blomqvist, Professor B. R. Mottelson, and Professor A. Arima for stimulating discussions. Finally, he expresses his gratitude to Professor I. Perlman and Professor J. O. Rasmussen for their hospitality at the Lawrence Radiation Laboratory.

PHYSICAL REVIEW C VOLUME 1, NUMBER 1 JANUARY 1970

# Lifetimes and Nuclear Moments in Os$^{192}$ and Pt$^{192}$

R. Béraud, I. Berkes, R. Chéry, R. Haroutunian, Michèle Lévy, G. Marguier, G. Marest, and R. Rougny
*Institut de Physique Nucléaire, Université de Lyon-I, 69-Villeurbanne, France*

(Received 24 July 1969)

Lifetimes, nuclear $g$ factors, and $E2/M1$ mixing ratios have been determined in Os$^{192}$ and Pt$^{192}$, and some previous determinations reevaluated. The following values have been established. For Os$^{192}$: $g_2=+0.29\pm0.05$; $\delta(484)=+7.6_{-1.3}^{+2.4}$. For Pt$^{192}$: $\tau_2=50.0\pm3.4$ psec; $\tau_2{}'=29\pm3$ psec; $g_2=+0.296\pm0.022$; $g_2{}'=+0.29\pm0.05$; $\delta(604)=+2.5\pm0.2$; $\delta(308)=-6.3_{-0.6}^{+0.5}$. Nuclear magnetic moments are analyzed in terms of Greiner's vibrational-rotational model, transition probabilities and $E2/M1$ mixing ratios are compared to the theoretical predictions of Kumar and Baranger's model.

## I. INTRODUCTION

The application of internal magnetic fields in iron alloys enables one to determine a great number of short-lived excited-state nuclear magnetic moments. Lifetime and nuclear moment data (until August 1967) are summarized in Ref. 1. The results on the first excited states in Pt nuclei show $g\simeq+0.3$; in Os$^{192}$ the results on the first excited state are contradictory. Moreover, $g$ factors of second excited 2$^+$ states are very scarce: for Dy$^{160}$, $g_{2'}=+0.18\pm0.06$[2]; for Os$^{188}$, $g_{2'}=+0.43\pm0.08$ [3] or $+0.57\pm0.14$,[4] reevaluated with recent lifetime and internal field data by Shirley[1]; and for Pt$^{194}$, $g_{2'}=+0.15\pm0.04$.[5,6]

Our knowledge on lifetimes of second excited states in Pt nuclei is also very poor. The lifetime of Pt$^{192}$, determined by delayed coincidence of conversion electrons $\tau_{2'}=34\pm19$ psec,[7] has a large error; that of Pt$^{194}$, estab-

[1] *Hyperfine Structure and Nuclear Radiations*, edited by E. Matthais and D. A. Shirley (North-Holland Publishing Co., Amsterdam, 1968).

[2] R. Simon, I. Arens, R. S. Raghavan, and H. J. Körner, Phys. Letters **28B**, 590 (1968).

[3] J. Murray, T. A. McMath, and J. A. Cameron, Can. J. Phys. **45**, 1597 (1967).

[4] L. Keszthelyi, I. Demeter, I. Dézsi, and L. Pócs, Nucl. Phys. **A91**, 692, (1965).

[5] L. Keszthelyi, I. Berkes, I. Dézsi, and L. Pócs, Nucl. Phys. **71**, 662 (1965).

[6] Y. K. Agarwal, C. V. K. Baba, and S. K. Bhattacherjee, Nucl. Phys. **79**, 437 (1966).

[7] D. K. Butt and D. A. Jackson, Proc. Phys. Soc. (London) **86**, 31 (1965).